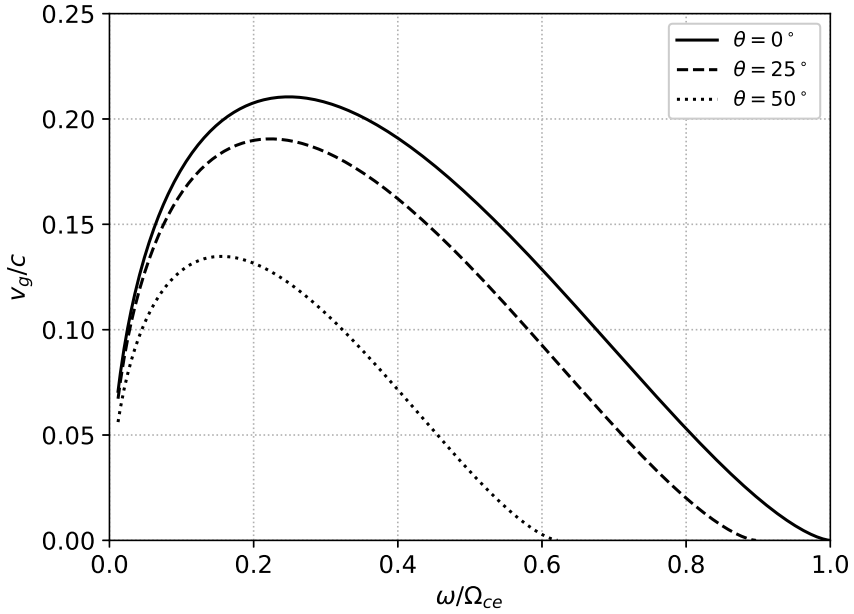

Figure 1. Group velocity v_g/c as a function of whistler-mode chorus waves frequency to the plasma gyrofrequency for three different wave normal angles propagation. This group velocity is the full solution of Appleton-Hartree for whistler waves propagating in low-density plasma media at any orientation. Plasma parameters used in the calculation are provided by the Van Allen Probes apogee orbit, $B_0 = 150$ nT, and low density $n = 2\ \mathrm{cm}^{-3}$.

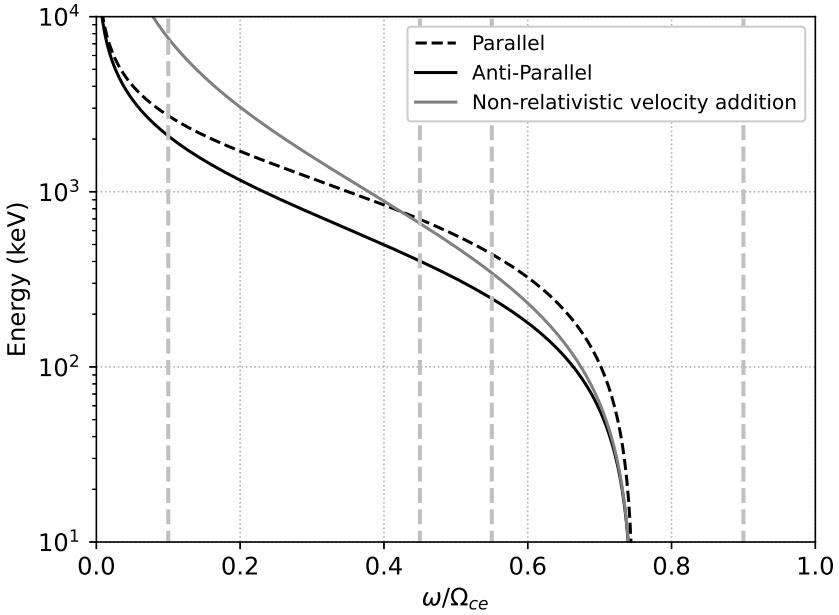

Figure 2. Comparison of the electron resonant kinetic energy (KeV) as a function of whistler-mode chorus wave frequency normalized by the electron gyrofrequency propagating parallel and anti-parallel to the ambient magnetic field ($B_0 = 150nT$). The wave-particle resonance condition depends on the wave dispersion relation ($\omega/\boldsymbol{k}$), calculated from Eq.2, with n = +5. The vertical lines delimitate the low-band whistler mode chorus wave frequency correspondent to $0.1f_{ce} \leq f \leq 0.45f_{ce}$ and the high-band $0.55f_{ce} \leq f \leq 0.90f_{ce}$ as a fraction of the electron gyrofrequency. Plasma parameters are the same as used in Figure 1

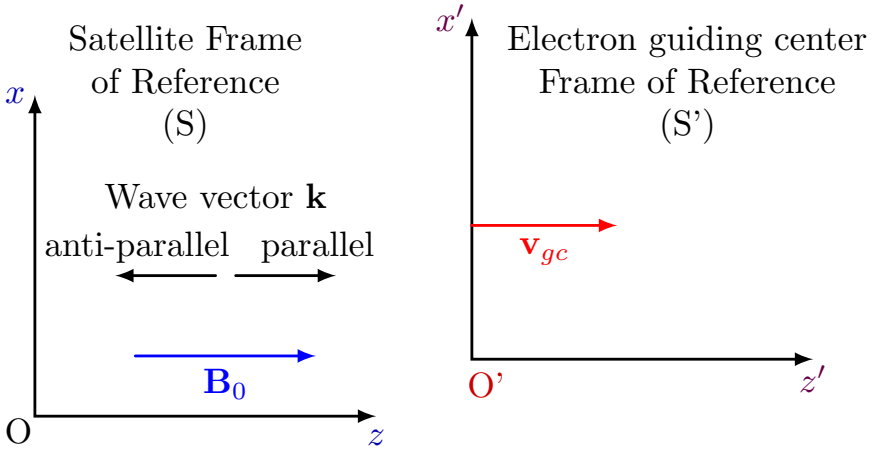

Figure 3. Here we illustrate the two reference frames used in calculating the interaction time in Section 3. The electron guiding center frame of reference (S') has a velocity $\boldsymbol{v}_{gc}$ with respect to the satellite frame of reference (S). This velocity parallels the ambient magnetic field $\boldsymbol{B}_0$. Thus, the angle between the wave vector $\boldsymbol{k}$ and $\boldsymbol{v}_{gc}$ equals the WNA given by θ.

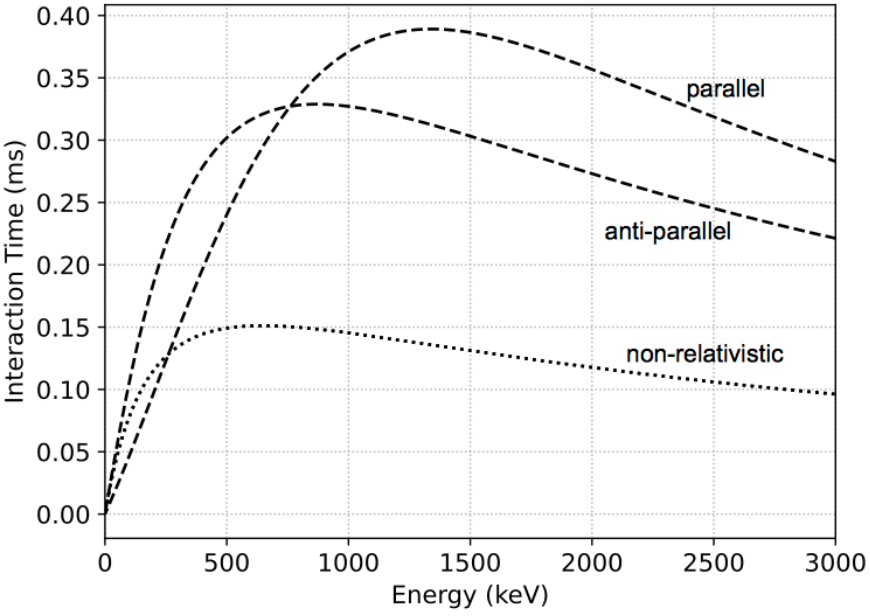

Figure 4. Comparison of time of interaction (ms) as a function of electron resonant kinetic energy (keV) calculated using Eq. (13) (dashed lines) and non-relativistic approach (dotted line) for parallel and anti-parallel wave propagation. Plasma parameters are: $B_{am} = 166$ nT, $\tau = 1.8$ ms, $n_e = 3.0cm^{-3}$

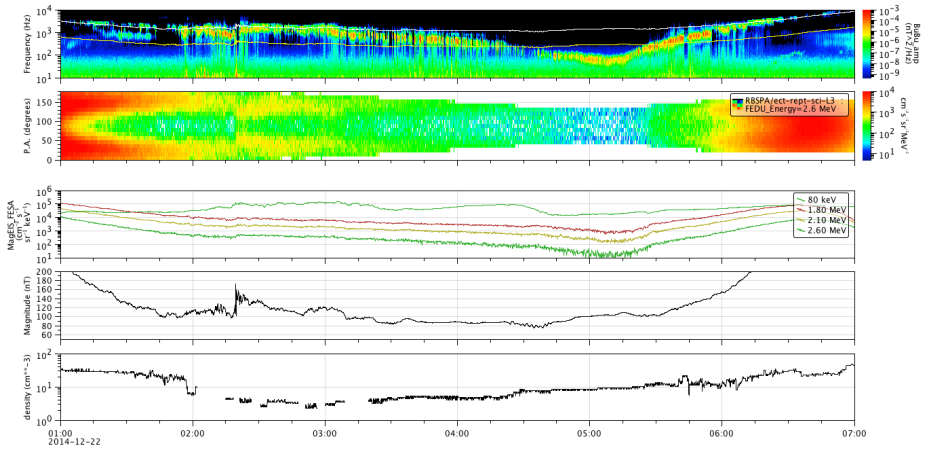

Figure 5. Panels show from top to bottom the whistler-mode chorus waves spectrum, the interpolated 1.8 MeV electron flux pitch angle distribution, the relativistic and low energy electron fluxes, the ambient magnetic field, and the local plasma density. The parameters shown in regions 3 and 4 were used to calculate the interaction time, change in pitch angle, and diffusion coefficient for the resonant electrons energy shown in Table 1

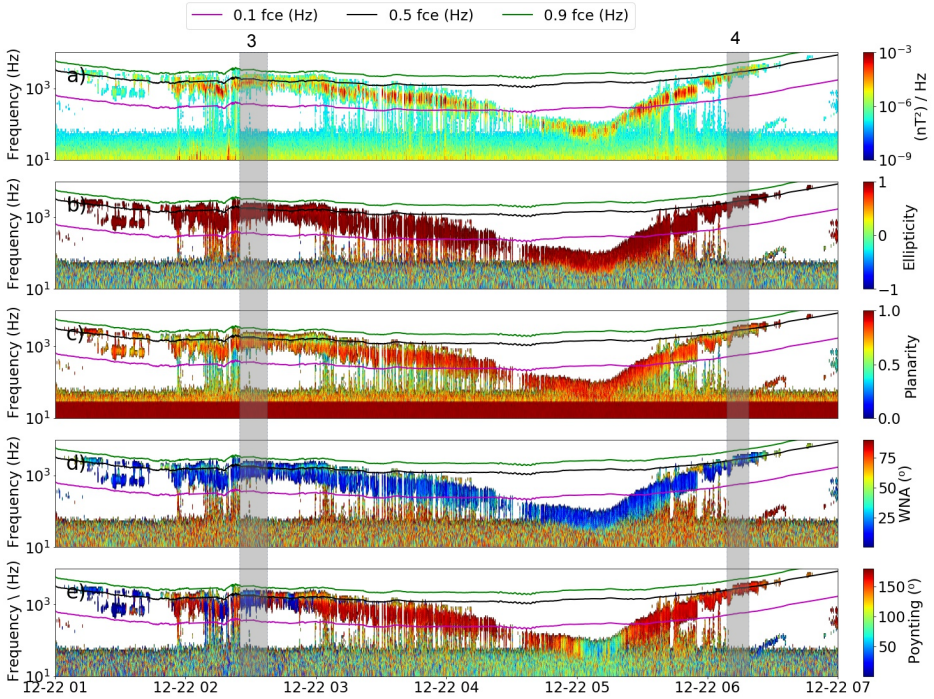

Figure 6. Panels show the whistler-mode chorus waves (a) spectrum of the magnetic field, (b) ellipticity; (c) planarity; (d) WNA – wave Normal angle; (e) the polar angle of Poynting vector. In all panels, the values of 0.1fce (Hz), 0.5fce (Hz), and 0.9 fce (Hz) are shown by the pink, black, and green lines, respectively. The parameters shown in regions 3 and 4 were used to calculate the interaction time, change in pitch angle and diffusion coefficient for the resonant electrons energy shown in Table 1

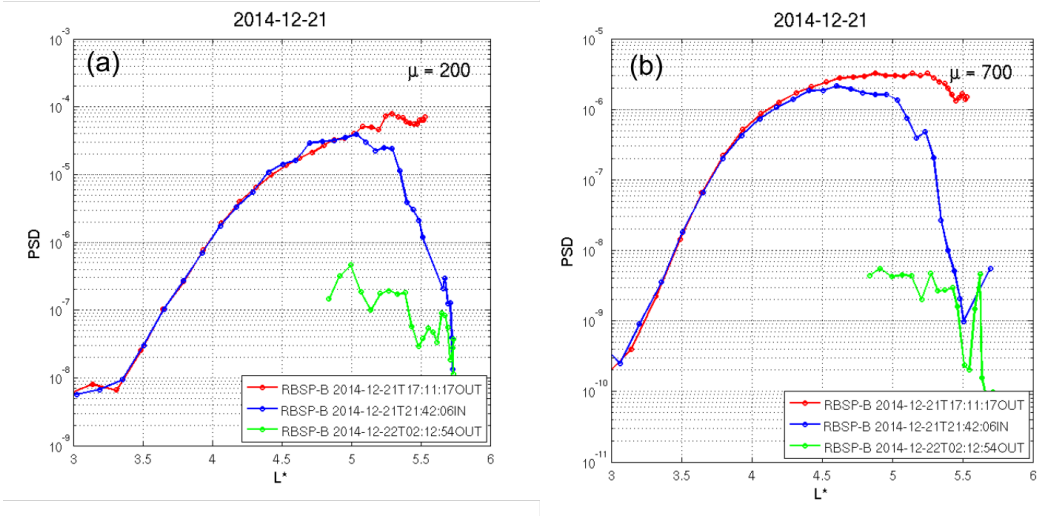

Figure 7. Time evolution of phase space density (PSD [c/(cm MeV))3 sr-1]) radial profiles at fixed first adiabatic invariant, μ=200MeV/G (a) and μ=200MeV/G (b), and second (K=0.11G1/2RE) adiabatic invariant for both inbound and outbound parts of the RBSP-B orbit. Period of analyzes: 21 Dec 2014 at 17:11:17 UT to 22 Dec 2014 at 02:12:54 UT.

Table 1. Input parameters used in the Equations of sections 2, 3, and 4 to calculate the chorus wave-particle time of interaction and the pitch angle diffusion coefficient for cases 1 to 4. $K_{res} = 1$ MeV and the initial equatorial pitch angle is 60°. For each case, the first (second) line shows results for parallel (antiparallel) propagating wave and electron. The subscript r and nr means relativistic and non-relativistic, respectively.

Input parameters					Results			
Cases	B_0 [nT]	n_e $[cm^{-3}]$	B_w [nT]	τ [ms]	T_r [ms]	T_{nr} [ms]	D_{aa} $[s^{-1}]$	D_{aa}^{nr} $[s^{-1}]$
1	234	2.3	0.16	0.2	0.04	0.02	7.87	1.67
					0.03	0.01	4.32	0.80
2	166	3.0	0.20	1.80	0.37	0.14	9.1	1.68
					0.33	0.14	6.8	2.76
3	112	9.1	0.40	2.0	0.10	0.06	2.09	1.45
					0.11	0.06	2.55	1.28
4	86	4.3	0.24	5.0	0.41	0.16	1.95	0.54
					0.42	0.16	2.08	0.43

Cases 1 (Tu et al., 2014) - from 8 October 2012 (dropout). Cases 3 and 4 (Liu et al., 2020) - 22 December 2014, 00:00 - 06:00 (UTC)

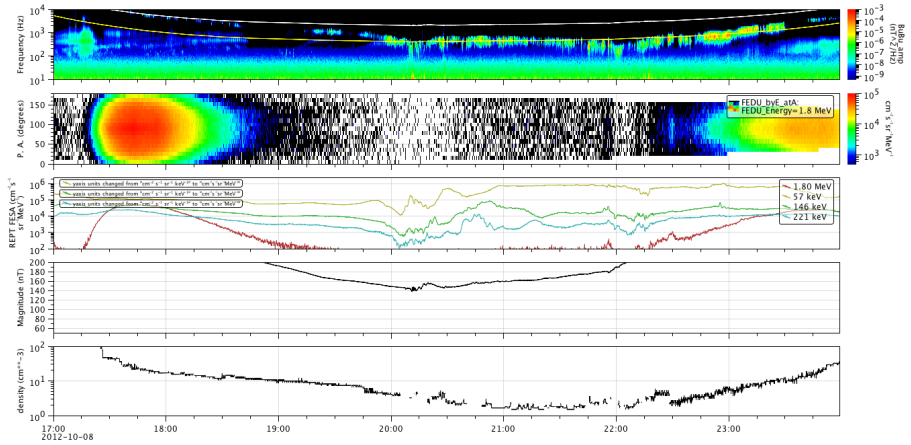

Figure A1. Panels show from top to bottom the whistler-mode chorus waves spectrum, the interpolated 1.8 MeV electron flux pitch angle distribution, the relativistic and low energy electron fluxes, the ambient magnetic field, and the local plasma density for the whistler mode chorus waves observed on 08 October 2012. The parameters shown in the highlighted area were used to calculate the time of interaction and change in pitch angle for the energy of the resonant electrons shown in Table 1.

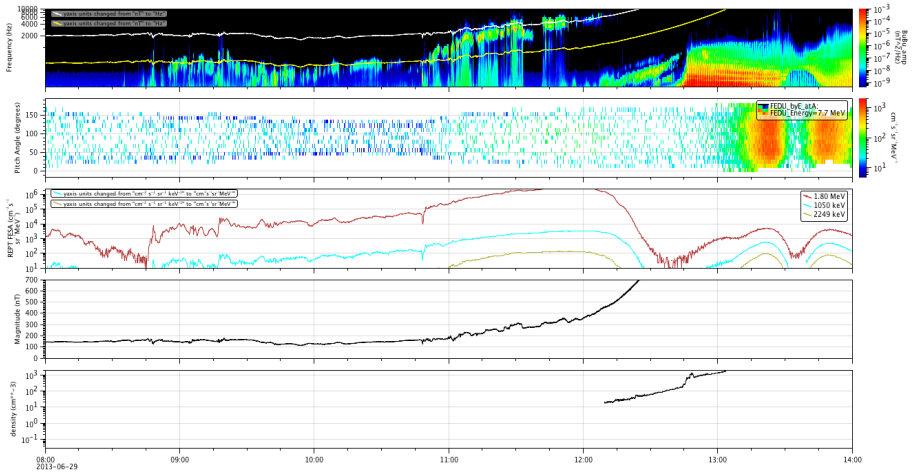

Figure B1. Panels show from top to bottom the whistler-mode chorus waves spectrum, the interpolated 1.8 MeV electron flux pitch angle distribution, the relativistic and low energy electron fluxes, the ambient magnetic field, and the local plasma density observed on 08 October 2012. The parameters shown in the highlighted area were used to calculate the time of interaction and change in pitch angle for the energy of the resonant electrons shown in Table 1.

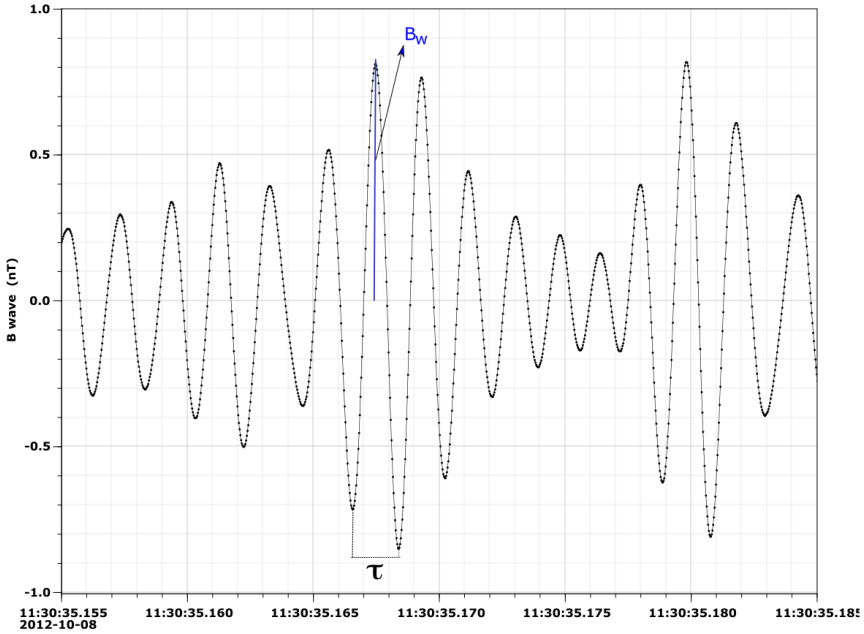

Figure C1. The high-resolution magnetic field measurement related to the event on 08 Oct 2012 during the higher magnetic field spectral density shown in Figure B1. The same plot was made for the other three studied events. The figure identifies the maximum instantaneous wave magnetic field amplitude B_w and the one wave cycle period τ.

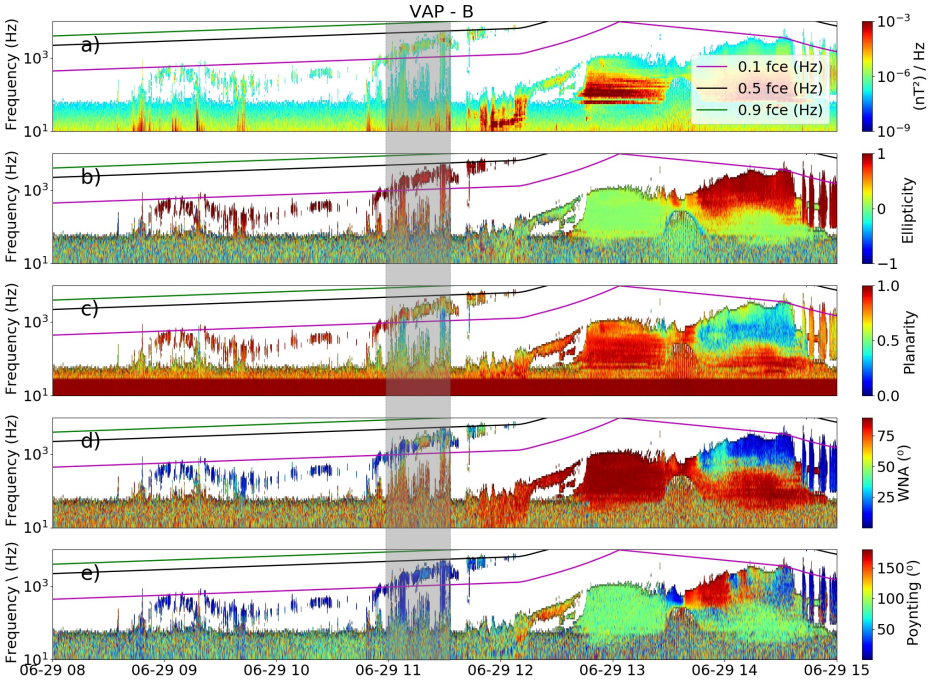

Figure D1. Panels from 29 Jun 2013, Case 2, show the whistler-mode chorus waves (a) spectrum of the magnetic field, (b) ellipticity; (c) planarity; (d) WNA – wave Normal angle; (e) the polar angle of Poynting vector. In all panels, the t values of 0.1fce (Hz), 0.5fce (Hz), and 0.9 fce (Hz) are shown by the pink, black, and green lines, respectively. The parameters shown from the gray shaded period are used to calculate the time of interaction and change in pitch angle for the resonant electrons energy shown in Table 1.

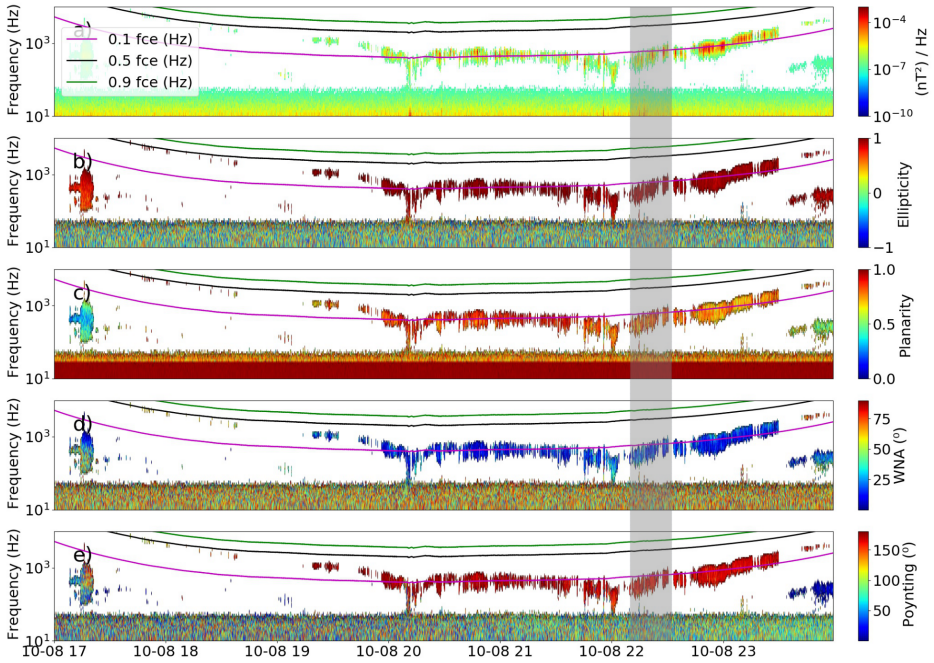

Figure E1. Same as Figure D1 for 08 October 2012, Case 1

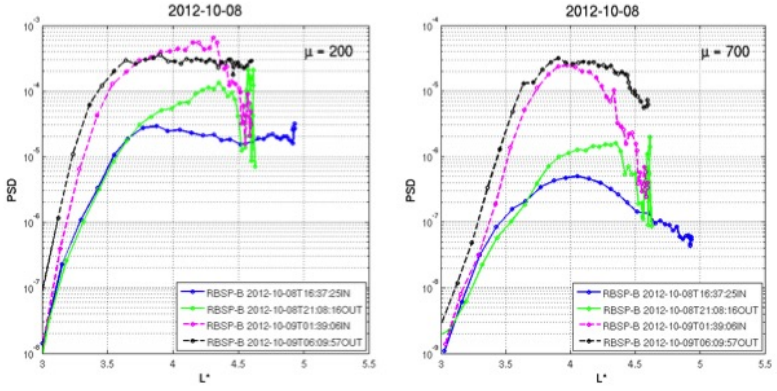

Figure F1. Time evolution of phase space density (PSD) radial profiles at fixed first adiabatic invariant, μ=200MeV/G (a) and μ=200MeV/G (b), and second (K=0.11G1/2RE) adiabatic invariant for both inbound and outbound parts of the RBSP-B orbit. Period of analyses: 08 Oct 2012 from 16:37 UT through the interval of interest

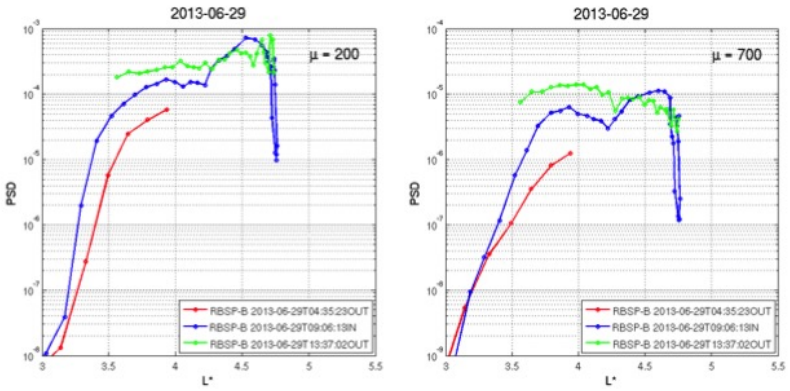

Figure G1. Same as Figure F1 for the period of analyses: 29 Jun 2012 through the interval of interest.